



*Supplement of*

## **Low confidence in multi-decadal trends of wind-driven upwelling across the Benguela Upwelling System**

**Mohammad Hadi Bordbar et al.**

*Correspondence to:* Mohammad Hadi Bordbar ([hadi.bordbar@io-warnemuende.de](mailto:hadi.bordbar@io-warnemuende.de), [ocean.circulation@gmail.com](mailto:ocean.circulation@gmail.com))

The copyright of individual parts of the supplement might differ from the article licence.

## ERA-5 data validation

Similar to ERA5 products, ASCAT has  $0.25^{\circ} \times 0.25^{\circ}$  spatial resolutions. This data set is based on the composites from records of three days. ASCAT provides observed near-real-time wind at 10-m height above the sea surface with almost global coverage. ASCAT data sets are publicly accessible. ERA5 reanalysis is derived from different resources, whereas ASCAT data is retrieved from satellite measurements.

The monthly mean ERA5 SLP closely correlates with the in situ-based SLP in St. Helena Island (Fig. S1). To validate the ERA5 winds, we compared the daily average of the meridional component of surface wind in ERA5 and ASCAT products for seven upwelling cells, including Kunene, Cape Frio, Walvis Bay, Lüderitz, Orange River, Hondeklip Bay, and Cape Columbine upwelling cells (Fig. S2). In general, there is a good agreement between ERA5 and ASCAT winds in all upwelling cells. Furthermore, the annual cycle of the meridional component of the surface wind along with the wind-stress-curl-driven (WSCD) upwelling in ERA5 and ASCAT during 2007-2021 are computed and compared (Fig. S3 and Fig. S4). Generally, the spatial patterns of annual cycles over the BUS agree reasonably well. Offshore ERA5 winds seem to be slightly underestimated. This is consistent with Belmonte Rivas and Stoffelen (2019), indicating that the underrepresentation of mid-latitude wind in ERA5 is potentially due to the model's low spatial resolution and lack of small-scale ocean processes (i.e., sub-mesoscale fronts and eddies). With more signatures off Kunene, Walvis Bay, and Cape Columbine, the WSCD upwelling in ERA5 appears to be slightly smaller than that derived from ASCAT. The spatial patterns of the ASCAT annual cycles generally feature more heterogeneity than the ERA5 dataset. The contour lines of the ERA5 meridional component of the wind velocity are smoother than that derived from ASCAT measurements (Fig. S3). The spatial pattern of long-term mean WSCD upwelling in the ASCAT is relatively noisy compared to that obtained from the ERA5. One should remember that ERA5 products are based on 12-hourly analysis centered at 06:00 and 18:00 UTC, whereas the ASCAT dataset is derived from the measurement when the satellite was overhead.

## Supplementary Figures

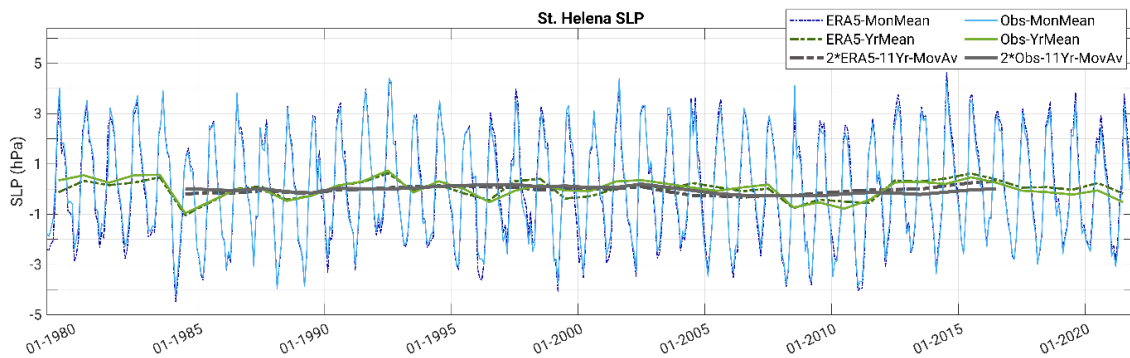


**Figure S1.** Time series of the monthly mean (blue lines), yearly mean (green lines), and 2×11-year running mean (dark grey lines) SLP (hPa) in St. Helena Island (5.7°W-15.95°S) derived from in situ measurement (solid lines) and ERA5 reanalysis (dash lines) from 1979-2021. The long-term mean SLP was subtracted from both time series. The ERA5 time series represent the areal average over a 1°×1° rectangular box (5°-6°W,15.50°-16.50°S) encompassing the island. Please note that the long-term mean SLP for the ERA5 and the observation is 1016.9 and 1017.8 hPa, respectively.

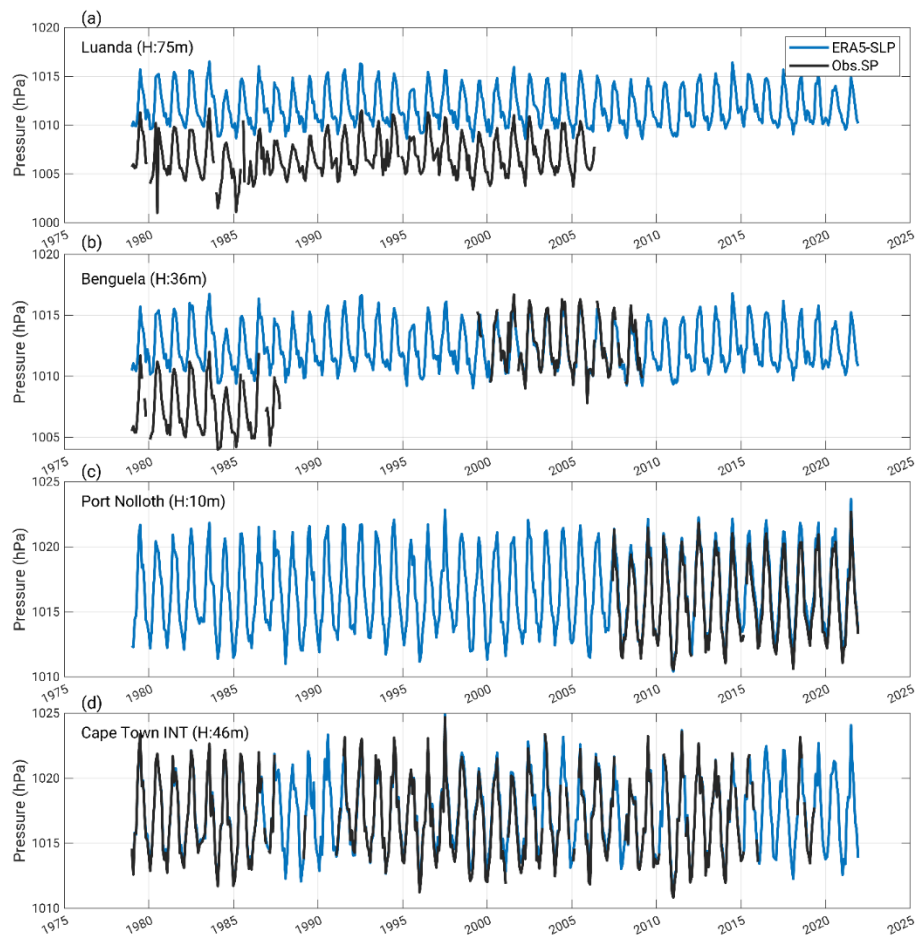


**Figure S2.** Time series of ERA5 monthly mean SLP (blue lines, hPa) and the observed surface pressure at climate stations (black lines, hPa). Panels a-d represent time series for Luanda (13.25°E, 8.85°S), Benguela (13.42°E,12.58°S), Port Nolloth (16.87°E,29.23°S), Cape Town International (18.60°E,33.96°S) stations, respectively. In each panel, the approximated altitude of the corresponding station from the global mean sea level is shown in the upper-left corner. The ERA5 SLPs were obtained from the areal average of 0.5°×0.5° rectangular boxes encompassing the location of the stations.

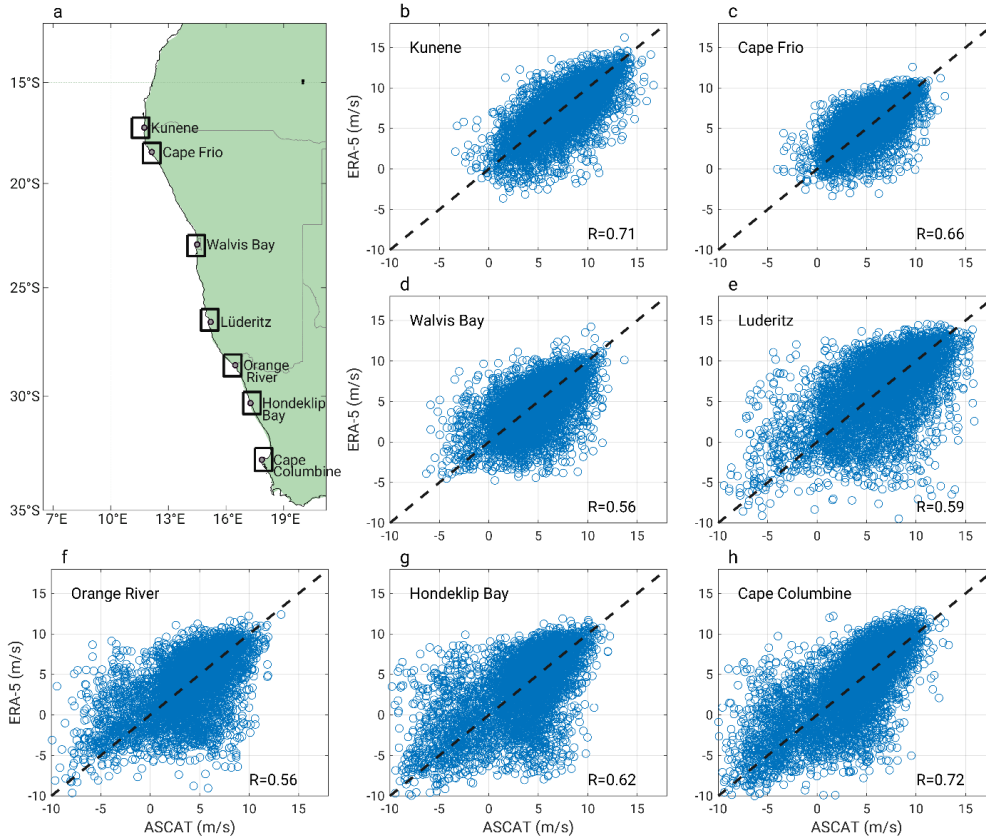


**Figure S3.** Daily mean ERA5 meridional surface wind (m/s) compared with ASCAT records for seven coastal upwelling cells across the BUS. The meridional wind was obtained from the areal averaged over the rectangular boxes shown in panel (a) and for 2007-2021. We flagged the wind data over the land as missing value and did not consider them. Panel b-h shows the results from the Kunene, Cape Frio, Walvis Bay, Lüderitz, Orange River, Hondeklip Bay, and Cape Columbine upwelling cells, respectively. The linear correlation ( $R$ ) between the ASCAT and ERA5 meridional winds is represented in the bottom-right corner of panels b-h.

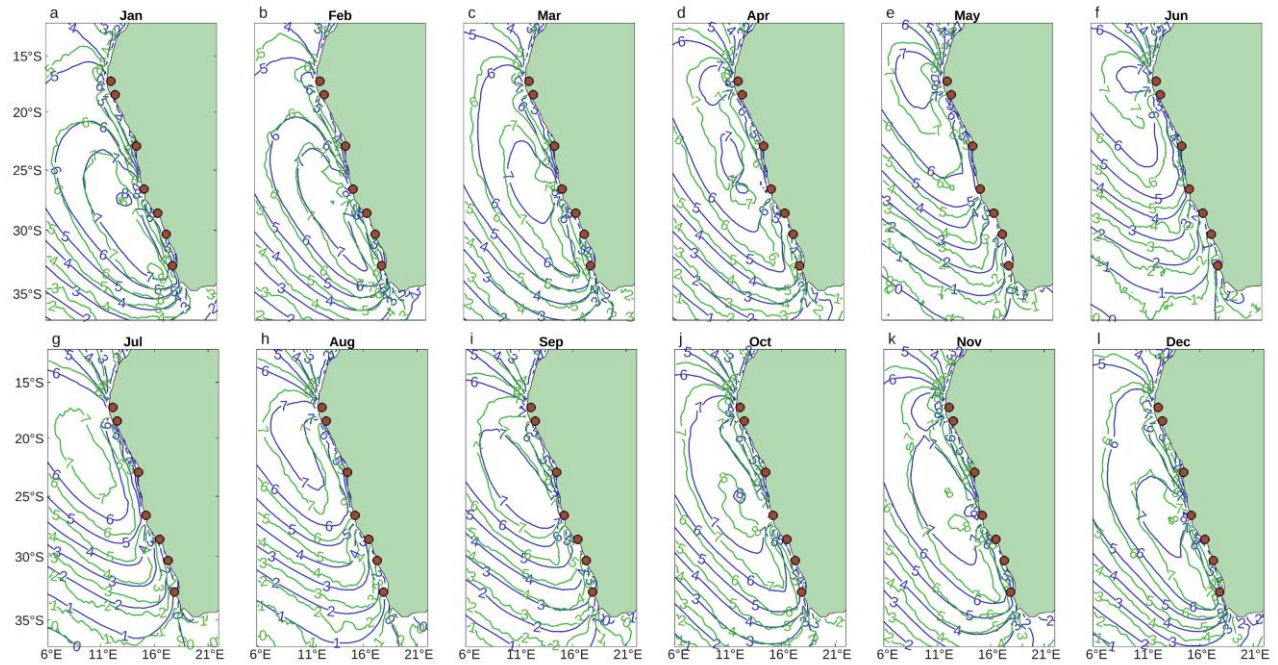


**Figure S4.** The annual cycles of the meridional wind velocity (m/s) over the southwest African coasts obtained from ERA-5 data (blue contours) and ASCAT records (green contours). The annual cycle computed over 2007-2021. Circles show the location of upwelling cells across the BUS, including Kunene, Cape Frio, Walvis Bay, Lüderitz, Orange River, Hondeklip Bay, and Cape Columbine cells.

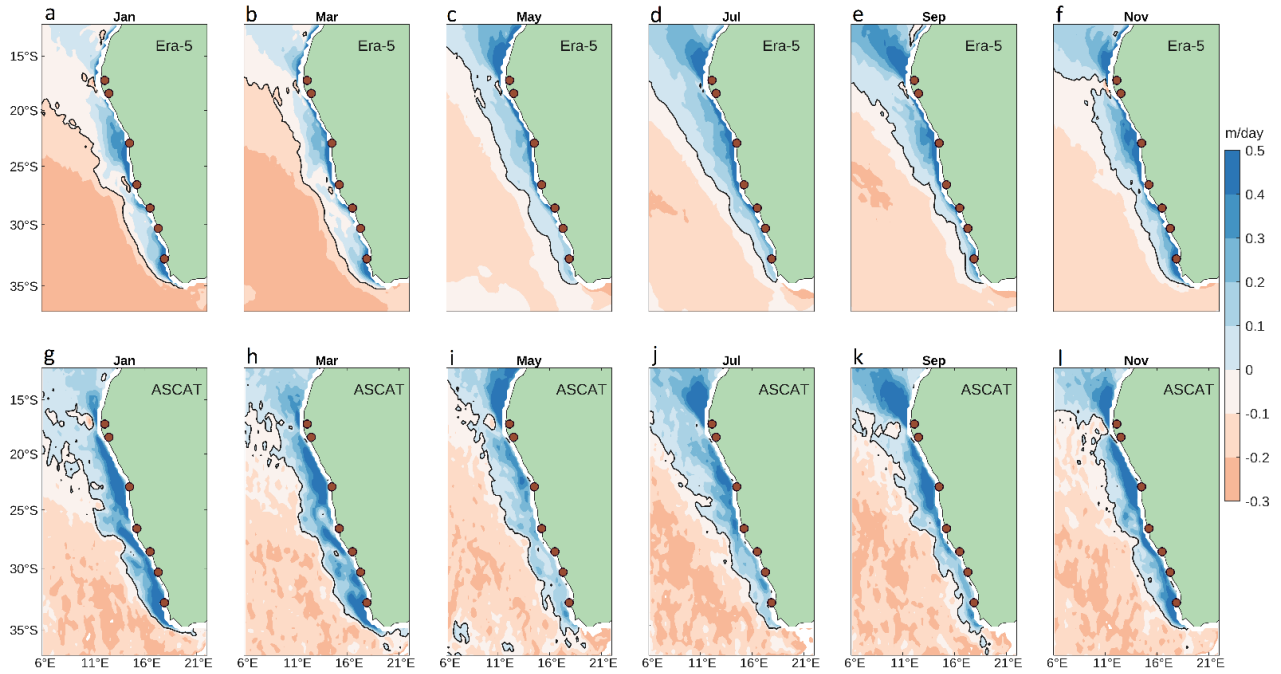


**Figure S5.** The annual cycles of the wind stress curl-driven upwelling (m/day) over the southwest African coast obtained from ERA5 data (top panels) and ASCAT measurements (bottom panels). The annual cycle computed over 2007-2021 and the values for January (a,g), March (b,h), May (c,i), July (d,j), September (e,k), and November (f,l) are shown here. Circles show the location of upwelling cells across the BUS.

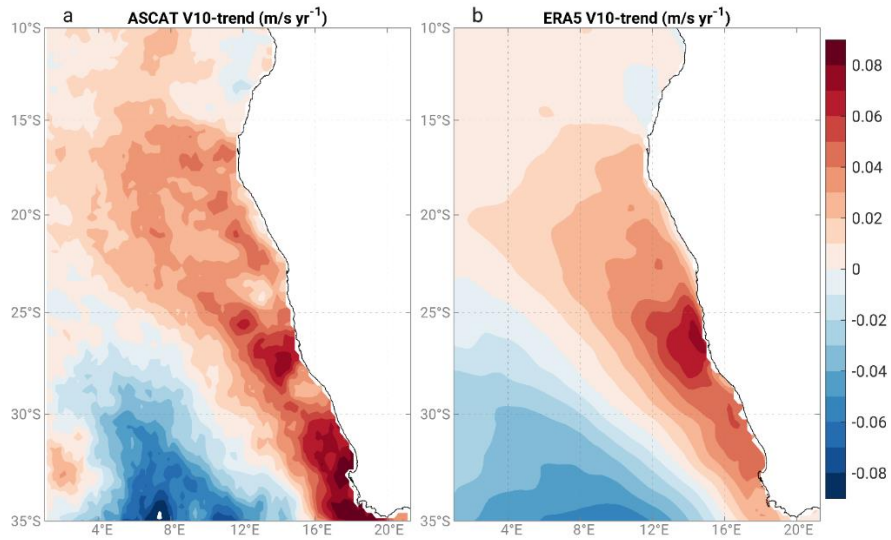


**Figure S6.** Linear trend ( $\text{m/s year}^{-1}$ ) in the meridional component of surface wind (V10) obtained from ASCAT (a) and ERA5 data (b) over 2008-2021.

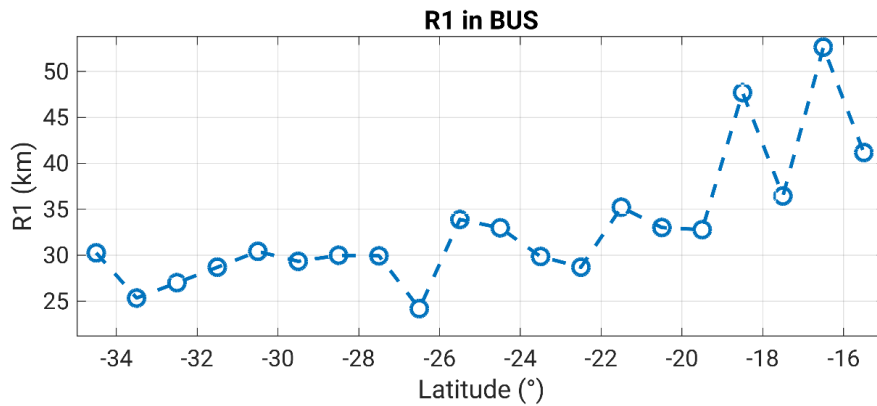


**Figure S7.** The first baroclinic Rossby radius of deformation ( $R_1$ ; km) over the coastal zone of BUS. Circles indicate the  $R_1$  from Chelton et al. (1998), and dashed line represents the interpolated  $R_1$  that is used in this study.

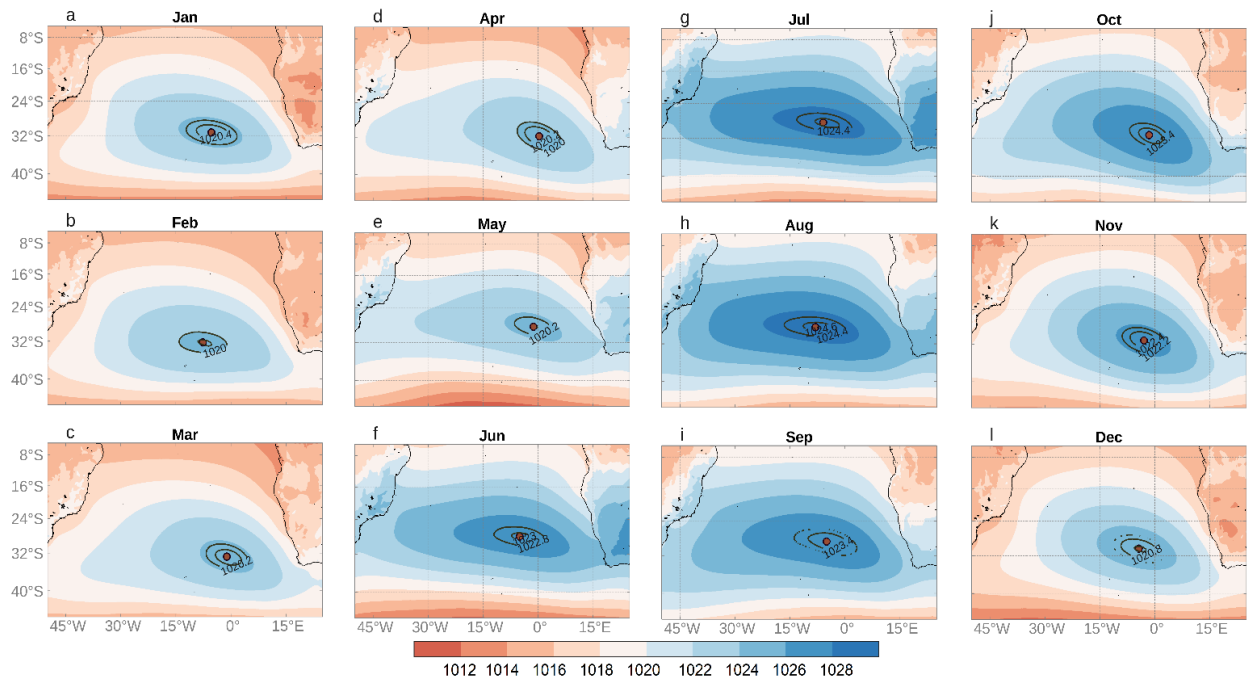


**Figure S8.** The annual cycle of the SLP (hPa) and the location of the SAA core (red circles) obtained from reanalysis over 1979-2021 (i.e., 43 years).



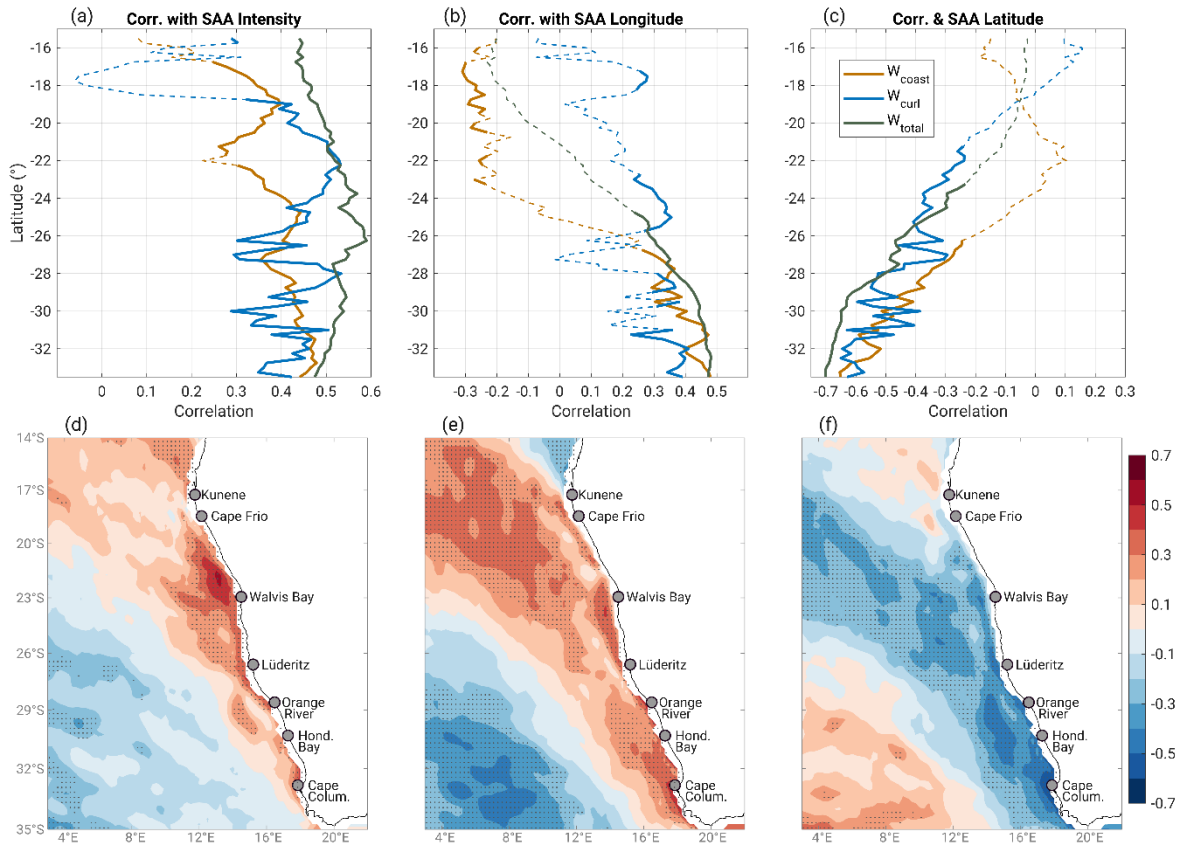


**Figure S9.** Same as figure 2, but anomaly correlation is computed for austral winter (i.e., Jun-Aug).

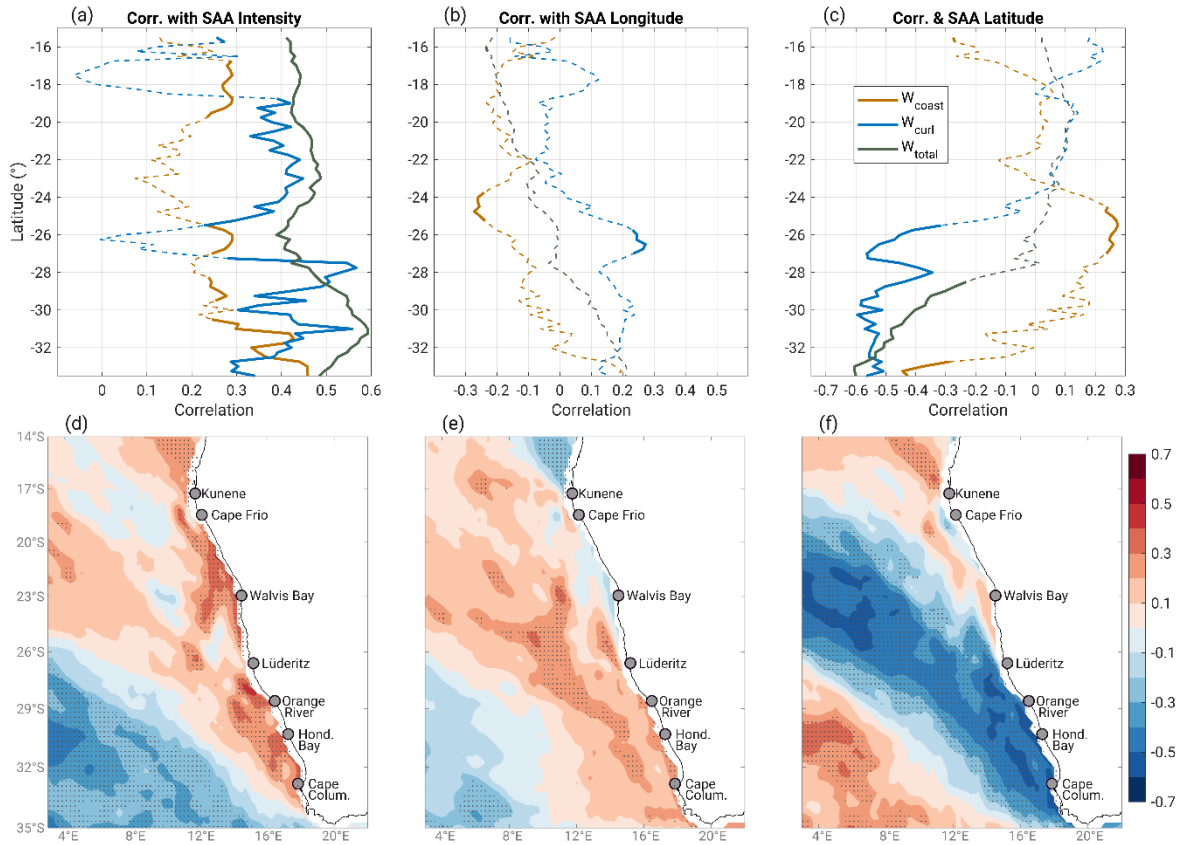
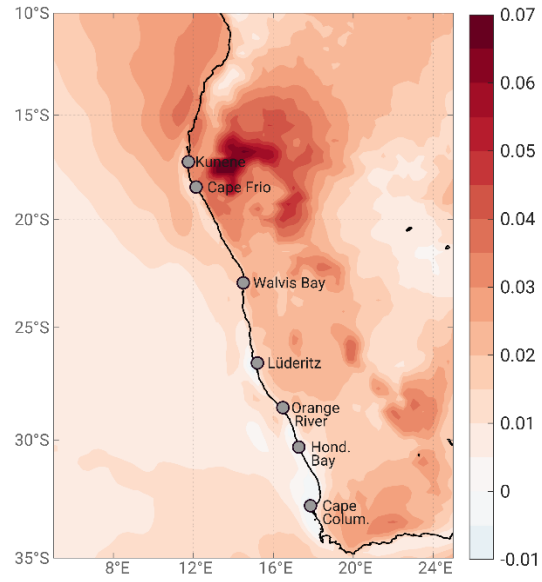
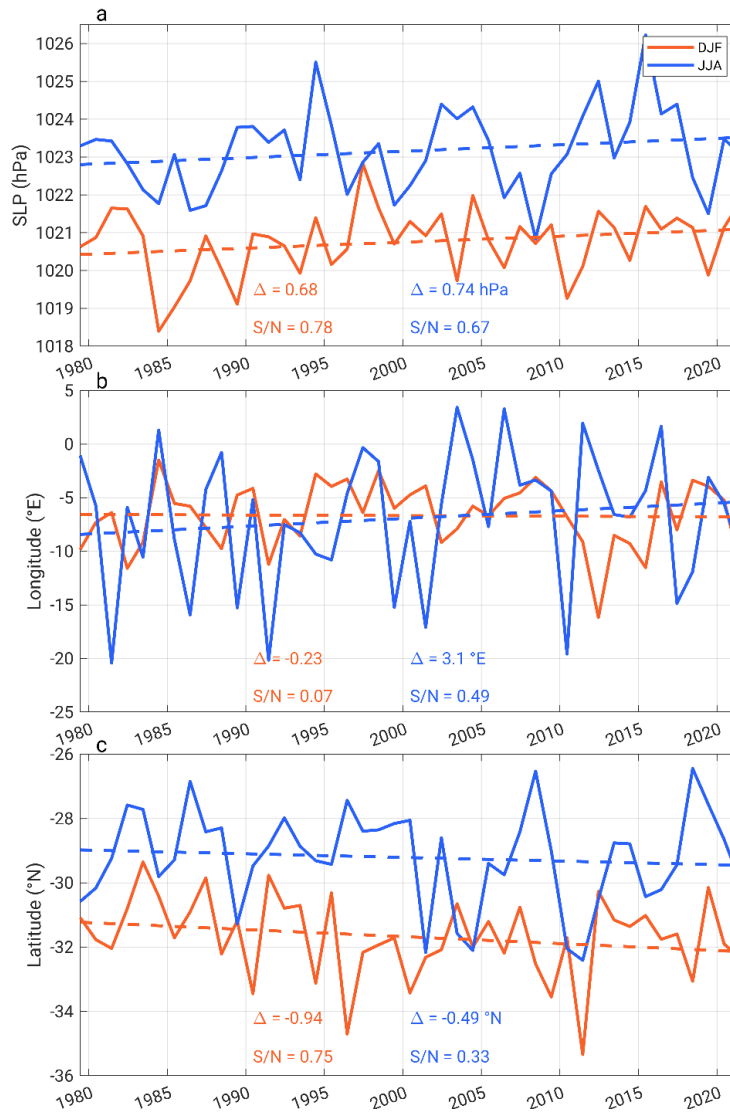


Figure S10. Same as figure 2, but anomaly correlation is computed for austral summer (i.e., Dec-Feb).



**Figure S11.** Linear trend in surface air temperature (°C/year) in the period of 1979-2021 derived from ERA5 data set.



**Figure S12.** Time evolution of summertime (Dec-Feb; red lines) and wintertime (Jun-Aug; blue lines) SAA intensity (a; hPa), longitude (b; °E) and latitude (c; °N) obtained from ERA5 for 1979–2021. The dashed lines indicate the trend line fitted to the time series. In each panel, time series, the  $\Delta$ , and S/N are shown by identical colors. Note that  $\Delta$  represents the changes associated with the linear trend over the entire period (i.e., 43-year).